

Universal classes of disorder scatterings in in-plane anomalous Hall effect

Guoao Yang,^{1,2} Tao Qin,^{1,*} and Jianhui Zhou^{2,†}

¹*School of Physics and Optoelectronics Engineering,
Anhui University, Hefei, Anhui Province 230601, P.R. China*

²*Anhui Provincial Key Laboratory of Low-Energy Quantum Materials and Devices,
High Magnetic Field Laboratory, HFIPS, Chinese Academy of Sciences, Hefei, Anhui 230031, China*
(Dated: January 7, 2025)

The in-plane anomalous Hall effect (IPAHE) with planar Hall current and magnetization/magnetic fields in various quantum materials has received increasing attentions. Most of current efforts are devoted to the intrinsic part due to the Berry curvature of electronic bands, however, how the disorder scatterings affect the extrinsic part (skew scattering and side jump) still remains largely elusive. Here we theoretically investigated the three universal classes of disorder scatterings (scalar, spin-conserving and spin-flipping) on the IPAHE based on the prototypical two-dimensional massive Dirac fermion model with warping term under generic Zeeman fields. We find the different disorder scatterings result in distinct dependence of the anomalous Hall conductivity on disorder strength and recover previous known results in some limits. Remarkably, the spin-flipping scattering could give rise to nontrivial contributions featuring sinusoidal oscillation with periods of π and 2π to the extrinsic part, in contrast to the standard two-dimensional massive Dirac fermions. Our work unveils the rich features of anomalous transport in planar Hall geometry in the presence of disorder scatterings and provides some useful insights into the magnetotransport phenomena.

I. INTRODUCTION

In contrast to the conventional anomalous Hall effect (AHE) with perpendicular Hall current and magnetization [1], the in-plane anomalous Hall effect (IPAHE) in which the Hall current and the magnetization are in the same plane has attracted much attentions due to the promising applications in low-energy electronics [2–17]. It originates from the Berry curvature of electrons and is generally attributed to the interplay between the magnetization and the spin-orbital interaction in magnetic materials [18]. Remarkably, the IPAHE has been experimentally observed in heterodimensional superlattice VS – VS₂ nanoflakes induced by an in-plane magnetic field [12, 14]. It further inspires the search for new materials hosting IPAHE and its detection in novel quantum materials [19–25].

The disorder scatterings that significantly modify the quasiparticles lifetime and phase and magnitude of velocity matrix elements play a vital role in transport properties of electrons in solids [26]. It is known that disorders could significantly change extrinsic contribution (skew scattering [27] and side jump [28]) of conventional AHE [29–37], which sometimes become comparable to or even predominant over the intrinsic contribution in kagome metal [38–40]. Current investigations of IPAHE mainly focus on the intrinsic part due to berry curvature of energy bands, however, the study of the extrinsic part due to the disorder scatterings is very rare [41]. In particular, how the inevitable spin-dependent scatterings by the magnetic disorders to affect IPAHE becomes crucial to understand the Hall transport experiments and to develop the energy-efficient electronic devices in magnetic materials.

In this work, we systematically investigate the impacts of the universality of disorder on the IPAHE by use of Kubo formula with 2D massive Dirac fermions with hexagonal warping term. We find that each universal class of scattering produces distinct behaviors of extrinsic part (the skew scattering and side jump) of AHE. We could recover previous results of AHE in conventional massive Dirac fermions in the presence of three universality classes of disorder and in Dirac fermions with warping term with nonmagnetic impurities. In addition, we calculate the in-plane magnetoresistance that enables us to well understand previous experimental results.

The rest of the work is organized as follows. In Sec. II, we briefly introduce the Dirac model with warping term under general Zeeman fields and calculate the intrinsic anomalous Hall conductivity. In Sec. III, we discuss the basic physics of three universal classes of disorder scatterings. Sec. IV presents the main results about the extrinsic AHC. In Sec. V, we calculate the in-plane magnetoresistance and make some comparison with previous results. Finally, we draw some conclusions.

II. MODEL FOR DIRAC FERMIONS WITH WARPING TERM

We consider the typical two-band model supporting the IPAHE and its quantized counterpart, which could be well described the surface states of a topological insulator with hexagonal warping term [3]

$$H_0(\mathbf{k}) = v(k_y\sigma_x - k_x\sigma_y) + \lambda_k\sigma_z + \mathcal{M} \cdot \hat{\sigma}, \quad (1)$$

where $\hat{\sigma} = (\sigma_x, \sigma_y, \sigma_z)$ are the Pauli matrices acting in the spin space, v is the Dirac velocity, and $\mathbf{k} = (k_x, k_y)$ is the 2D wave vector. The first term is the

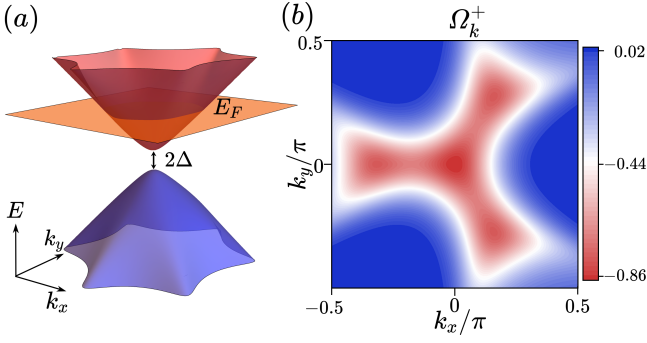


Figure 1. (a) Schematic of the energy band of the Dirac surface states of the topological insulator with the hexagonal warping. The Fermi energy lies in the conduction band. (b) The distribution of the Berry curvature of the conduction band with only out-of-plane magnetization \mathcal{M}_z in the momentum space, the parameters are given as $\lambda = 0.1 \text{ eV nm}^3$, $v = 0.2 \text{ eV nm}$, $\mathcal{M}_z = 0.15 \text{ eV}$.

Rashba type spin-momentum locking, the second term $\lambda_k = \lambda k_x(k_x^2 - 3k_y^2)$ is the generic hexagonal warping term [42], and the third term is the Zeeman coupling or the magnetization energy $\mathcal{M} = (\mathcal{M}_\parallel, \mathcal{M}_z)$ where $\mathcal{M}_\parallel = (\mathcal{M}_\parallel \cos \theta, \mathcal{M}_\parallel \sin \theta) = g\mu_B \mathbf{B}/2$ is the in-plane component and \mathcal{M}_z is the out-of-plane component. g the effective g factor and μ_B the Bohr magneton. The energy dispersion is of the form

$$\varepsilon_{\mathbf{k}}^\pm = \pm \varepsilon_{\mathbf{k}} = \pm \sqrt{v^2 q^2 + (\lambda_k + \mathcal{M}_z)^2}, \quad (2)$$

with $\mathbf{q} = (q_x, q_y) = [(-vk_y + \mathcal{M}_x)/v, (vk_x + \mathcal{M}_y)/v]$. The corresponding eigenstates are $\psi_{\mathbf{k}}^\pm(\mathbf{r}) = |u_{\mathbf{k}}^\pm\rangle e^{i\mathbf{k}\cdot\mathbf{r}}$ with

$$|u_{\mathbf{k}}^+\rangle = \begin{pmatrix} \cos \frac{\Theta_{\mathbf{k}}}{2} \\ \sin \frac{\Theta_{\mathbf{k}}}{2} e^{i\phi_{\mathbf{k}}} \end{pmatrix}, |u_{\mathbf{k}}^-\rangle = \begin{pmatrix} \sin \frac{\Theta_{\mathbf{k}}}{2} \\ -\cos \frac{\Theta_{\mathbf{k}}}{2} e^{i\phi_{\mathbf{k}}} \end{pmatrix}, \quad (3)$$

where $\Theta_{\mathbf{k}} = \tan^{-1} vq/(\lambda(k_x^3 + k_x k_y^2) + \mathcal{M}_z)$, $\phi = \tan^{-1} q_y/q_x$. The Zeeman coupling caused by the in-plane field shifts the Dirac point away from the point $\mathbf{k} \equiv 0$ to $\mathbf{k}' \equiv \hat{z} \times \mathcal{M}_\parallel/v$ [42], and the hexagonal warping term then opens a small gap $2\Delta_1 \equiv 2\lambda k'^3 \sin 3\theta$ at the Dirac point [43]. Similarly, the external magnetic field in the z -direction will also open the energy gap $2\Delta_2 \equiv 2\mathcal{M}_z$ of the system. The effective gap becomes $2\Delta \approx 2(\Delta_1 + \Delta_2)$, leading to a sizable AHE.

It is straightforward to evaluate the Berry curvature of the conduction band as

$$\Omega_{\mathbf{k}}^\pm = \frac{\pm v}{2\varepsilon_{\mathbf{k}}^3} [v(2\lambda_k - \mathcal{M}_z) + 3\lambda(\mathcal{M}_y(k_x^2 - k_y^2) + 2\mathcal{M}_x k_x k_y)]. \quad (4)$$

The integration of $\Omega_{\mathbf{k}}^\pm$ over the Brillouin zone gives rise to the intrinsic anomalous Hall conductivity in the leading order of warping parameter [Details can be found in

Supplemental Material [44]]

$$\sigma_{xy}^{in} = -\frac{e^2}{h} \left(\frac{\mathcal{M}_z}{2E_F} + \frac{\lambda \mathcal{M}_\parallel^3 \sin 3\theta}{2v^3 E_F} \right). \quad (5)$$

where θ is the angle between the in-plane magnetic field or magnetization and the x axis. The first contribution comes from the out-of-plane magnetic field or magnetization, while the second one is induced by the in-plane magnetic field that breaks the combination of time reversal symmetry and mirror symmetry. When the Fermi level lies in the band gap, the first term reduces to be the known half-quantized Hall conductivity [45]. Note that the high-order term corresponding to the magnetic octuple contribution and reflects the anisotropic Fermi surface due to the warping term with C_{3v} symmetry.

III. UNIVERSAL CLASSES OF DISORDER SCATTERINGS

In order to simulate the spin-dependent scatterings in magnetic materials, we consider the general form of a random disorder potential for carriers with spin (or pseudo-spin) degrees of freedom

$$\hat{V}_{dis}(\mathbf{r}) = \sum_i (V_0 \hat{\sigma}_0 + \mathbf{V} \cdot \hat{\boldsymbol{\sigma}}) \delta(\mathbf{r} - \mathbf{R}_i), \quad (6)$$

where \mathbf{R}_i ($i = 1, 2, \dots$) labels positions of randomly distributed scattering centers, and V_0 and $\mathbf{V} = (V_x, V_y, V_z)$ are strength of the magnetic impurity.

We focus on three different types of disorders. First, in ferromagnetic materials, normal (nonmagnetic) impurity scattering and phonon scattering belong to class A ($V_0 \hat{\sigma}_0$ type impurity). Second, the class B ($V_z \hat{\sigma}_z$ type impurity) refers to the scatterings of magnetic impurities that conserves the z component of the carrier spin. Third, the scattering processes of class C ($V_x \hat{\sigma}_x$ and $V_y \hat{\sigma}_y$ type impurities) are due to the spin-flipping scatterings by in-plane random magnetic impurities or the magnetic fluctuations of in-plane magnetic order [31, 46].

We assume that the statistical average of the disorder potential is zero since any nonzero value only shifts the origin of total energy, and that the second-order spatial correlation only depends on the difference in positions within the Gaussian approximation. Therefore, for different types of impurities listed above and calculations presented in the following, we have the zero average value $\langle V_{dis, \mathbf{k}, \mathbf{k}'}^{\eta \eta'} \rangle_{imp} = 0$, where $\eta, \eta' = \pm$ indicating matrix element between eigenstate η and η' , and the angular brackets $\langle \dots \rangle_{imp}$ denote disorder average [47]. We then have the Gaussian correlations between disorders,

$$\langle V_{\mathbf{k}, \mathbf{k}'}^{l, \eta \eta'} V_{\mathbf{k}', \mathbf{k}}^{m, \eta' \eta} \rangle_{imp}$$

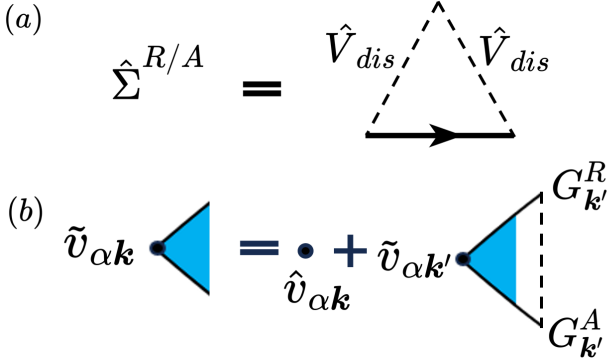


Figure 2. (a) The electron self-energy due to the impurity scatterings in the first Born approximation. (b) The vertex correction of the velocity operator $\tilde{v}_{\alpha\mathbf{k}}$ for calculating the electric conductivity $\sigma_{\alpha\beta}$.

$$= \frac{n_i u_0^2}{V} \langle u_{\mathbf{k}}^{\eta} | \sigma_l | u_{\mathbf{k}'}^{\eta'} \rangle \langle u_{\mathbf{k}'}^{\eta'} | \sigma_m | u_{\mathbf{k}}^{\eta} \rangle, \quad (7)$$

where $l, m = x, y, z$, n_i is the impurity concentration, and u_0 is the disorder strength in Gaussian approximation. Furthermore, in order to evaluate the impacts of the skew scattering due to anisotropic part of the scattering rate, we need to take into account at least the third-order disorder non-Gaussian correlations,

$$\begin{aligned} & \langle V_{\mathbf{k},\mathbf{k}'}^{l,\eta\eta'} V_{\mathbf{k}',\mathbf{k}''}^{m,\eta'\eta''} V_{\mathbf{k}'',\mathbf{k}}^{n,\eta''\eta} \rangle_{imp} \\ &= \frac{n_i u_1^3}{V^2} \langle u_{\mathbf{k}}^{\eta} | \sigma_l | u_{\mathbf{k}}^{\eta'} \rangle \langle u_{\mathbf{k}}^{\eta'} | \sigma_m | u_{\mathbf{k}''}^{\eta''} \rangle \langle u_{\mathbf{k}''}^{\eta''} | \sigma_n | u_{\mathbf{k}}^{\eta} \rangle, \quad (8) \end{aligned}$$

where u_1 is the disorder strength in non-Gaussian approximation. Next, we would separately calculate the anomalous Hall conductivity caused by three impurity scattering classes.

IV. EXTRINSIC ANOMALOUS HALL EFFECT

A. Kubo formula

The Kubo formula provides us with a systematic way to calculate the anomalous Hall conductivity in the weak scattering regime and reveals some fundamental features of AHE in magnetic materials [48],

$$\sigma_{xy}^{\text{total}} = \sigma_{xy}^{\text{I}} + \sigma_{H,xy}^{\text{II}}, \quad (9)$$

$$\sigma_{xy}^{\text{I}} = \frac{e^2 \hbar}{2\pi} \sum_{\mathbf{k}} \text{Tr} \langle \hat{v}_{x\mathbf{k}} G_{\mathbf{k}}^R \hat{v}_{y\mathbf{k}} G_{\mathbf{k}}^A \rangle_{imp}, \quad (10)$$

$$\sigma_{xy}^{\text{II}} = -\sigma_{yx}^{\text{II}} = ec \left. \frac{\partial n(E)}{\partial B} \right|_{E=E_F, B=0}. \quad (11)$$

The first term σ_{xy}^{I} describes the contribution of electrons in the conduction band near the Fermi surface while σ_{xy}^{II}

accounts for the contribution to the entire Fermi sea. Note that σ_{xy}^{II} has played a key role in understanding the topological nature of integer quantum Hall effect from the point view of thermodynamics.

To proceed, we calculate the averaged Green function by solving the Dyson equation in the first Born approximation as shown in Fig. 2(a), where the full retarded/advanced Green's functions are given by

$$G^{R/A} = \frac{1}{E_F - \hat{H} \pm i\Gamma}, \quad (12)$$

where $\Gamma = \Gamma_0 \sigma_0 + \Gamma_x \sigma_x + \Gamma_y \sigma_y + \Gamma_z \sigma_z$ is the imaginary part of the self energy $\Sigma^{R/A}$. The self energy in the first Born approximation is

$$\Sigma^{R/A} = \sum_{\mathbf{k}} \langle V_{dis} G_{\mathbf{k}}^{R/A} V_{dis} \rangle_{imp}. \quad (13)$$

Meanwhile, the vertex correction in the ladder approximation (in Fig. 2(b)) [29] at the Fermi energy is given by

$$\tilde{v}_{x/y\mathbf{k}} = \hat{v}_{x/y\mathbf{k}} + \sum_{\mathbf{k}'} \langle V_{dis} G_{\mathbf{k}'}^{A/R} \tilde{v}_{x/y\mathbf{k}'} G_{\mathbf{k}'}^{R/A} V_{dis} \rangle_{imp}, \quad (14)$$

which determines the corrected vertex function of $\tilde{v}_{\alpha\mathbf{k}}$ from the bare velocity operator $\hat{v}_{\alpha\mathbf{k}}$ with $\alpha = x, y$.

For electron conduction and up to the first order of λ at zero temperature and zeroth order of impurity concentration n_i , the total Hall conductivity can be calculated analytically in the spin basis or eigenstate basis [Details are given in Supplemental Material [44]].

$$\sigma_{xy} = (\sigma_{xy}^{in} + \sigma_{xy}^{sj,2} + \sigma_{xy}^{sk,4}) + \sigma_{xy}^{sk,3}. \quad (15)$$

In this work, we are mostly interested in the Hall conductivity σ_{xy} of the order n_i^0 ($\sigma_{xy}^0 = \sigma_{xy}^{in} + \sigma_{xy}^{sj,2} + \sigma_{xy}^{sk,4}$) and of the order n_i^{-1} ($\sigma_{xy}^{-1} = \sigma_{xy}^{sk,3}$). Here we follow the conventions in Ref. [29].

B. Side jump part

We first calculate the contribution of the side jump contribution through the Kubo formula approach. In the semiclassical picture, the side jump we defined here consists of three components: the coordinate shift, a correction of the distribution function, and some higher order scattering processes (the intrinsic skew scattering) [29]. Fig. 3(a) shows a set of diagrams that contribute to the intrinsic and side jump in the spin basis. The contribution to Hall conductivity from second order side jump contribution for each scattering class is $\sigma_{xy}^{sj,2}$, and the contribution of the fourth-order scattering processes (intrinsic skew scattering) is $\sigma_{xy}^{sk,4}$. Then the total side jump

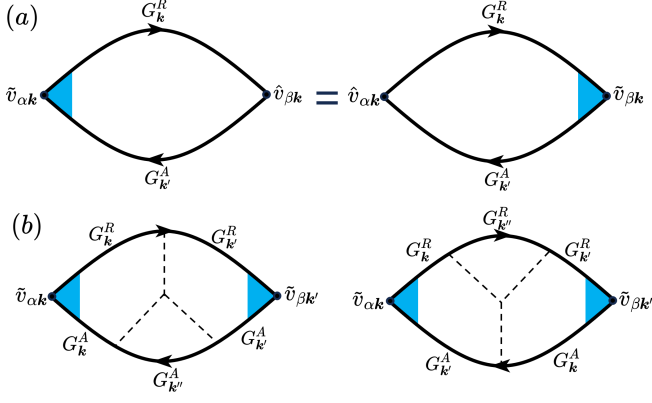


Figure 3. The Feynman diagrams for calculating the electric conductivity tensor $\sigma_{\alpha\beta}$. (a) Total conductivity of order n_{dis}^0 , (b) Total conductivity of order n_{dis}^{-1} .

contribution to anomalous Hall conductivity is given by $\sigma_{xy}^{sj} = \sigma_{xy}^{sj,2} + \sigma_{xy}^{sk,4}$.

Class A :

$$\begin{aligned} \sigma_{xy, V_0}^{sj} &= \frac{e^2}{h} \left(\frac{\mathcal{M}_z}{2E_F} - \frac{4E_F \mathcal{M}_z (E_F^2 + \mathcal{M}_z^2)}{(E_F^2 + 3\mathcal{M}_z^2)^2} \right) \\ &+ \left(1 - \frac{8E_F^2 (E_F^4 - 6E_F^2 \mathcal{M}_z^2 - 3\mathcal{M}_z^4)}{(E_F^2 + 3\mathcal{M}_z^2)^3} \right) \\ &\times \frac{e^2 \lambda \mathcal{M}_{\parallel}^3 \sin 3\theta}{h 2v^3 E_F}. \end{aligned} \quad (16)$$

Class B :

$$\begin{aligned} \sigma_{xy, V_z}^{sj} &= \frac{e^2}{h} \left(\frac{\mathcal{M}_z}{2E_F} - \frac{4E_F \mathcal{M}_z (E_F^2 + \mathcal{M}_z^2)}{(3E_F^2 + \mathcal{M}_z^2)^2} \right) \\ &+ \left(1 - \frac{8E_F^2 (3E_F^4 + 6E_F^2 \mathcal{M}_z^2 - \mathcal{M}_z^4)}{(3E_F^2 + \mathcal{M}_z^2)^3} \right) \\ &\times \frac{\lambda \mathcal{M}_{\parallel}^3 \sin 3\theta}{2v^3 E_F}. \end{aligned} \quad (17)$$

Class C :

$$\sigma_{xy, V_x}^{sj} = \frac{e^2}{h} \left(\frac{\mathcal{M}_z}{2E_F} - \frac{2\lambda E_F \mathcal{M}_{\parallel} \sin \theta}{v^3} + \frac{\lambda \mathcal{M}_{\parallel}^3 \sin 3\theta}{2v^3 E_F} \right). \quad (18)$$

$$\sigma_{xy, V_y}^{sj} = \frac{e^2}{h} \left(\frac{\mathcal{M}_z}{2E_F} + \frac{2\lambda E_F \mathcal{M}_{\parallel} \sin \theta}{v^3} + \frac{\lambda \mathcal{M}_{\parallel}^3 \sin 3\theta}{2v^3 E_F} \right). \quad (19)$$

There are several features of the side jump contributions. First, for all of three classes, they are independent of disorder density and scattering strength, similar to the pure intrinsic AHE. Second, the side jump contributions contain two parts from the out-plane magnetization \mathcal{M}_z and in-plane one \mathcal{M} and exhibit distinct dependence of

magnetization. It may originate from the different self-energy and k -dependence of scattering vertices. Third, the threefold rotational symmetry is preserved in the contribution from the in-plane magnetization in the first two classes (A and B) but gets broken in the class C. Noted that in the class C, combining with intrinsic one, leaving the only part with a 2π period.

C. Skew scattering part

We turn to calculate the skew scattering contribution for each scattering class. Fig. 3(b) show a set of diagrams that contribute to the skew scattering in the spin basis. The skew scattering contribution comes from the asymmetric part of the scattering rates for higher order scattering processes [27], and its contribution to anomalous Hall conductivity depends on disorder density and scattering strength:

$$\begin{aligned} \text{Class A : } \sigma_{xy, V_0}^{sk} &= -\frac{e^2}{h} \frac{u_1^3}{n_i u_0^4} \mathcal{M}_z \frac{(E_F^2 - \mathcal{M}_z^2)^2}{(E_F^2 + 3\mathcal{M}_z^2)^2} \\ &- \frac{e^2}{h} \frac{u_1^3}{n_i u_0^4} \frac{\lambda \mathcal{M}_{\parallel}^3 \sin 3\theta}{v^3} \frac{(E_F^2 - \mathcal{M}_z^2)}{(E_F^2 + 3\mathcal{M}_z^2)^3} \\ &\times (E_F^4 - 14E_F^2 \mathcal{M}_z^2 - 3\mathcal{M}_z^4). \end{aligned} \quad (20)$$

$$\begin{aligned} \text{Class B : } \sigma_{xy, V_z}^{sk} &= \frac{e^2}{h} \frac{u_1^3}{n_i u_0^4} E_F \frac{(E_F^2 - \mathcal{M}_z^2)^2}{(3E_F^2 + \mathcal{M}_z^2)^2} \\ &- \frac{e^2}{h} \frac{u_1^3}{n_i u_0^4} \frac{16\lambda \mathcal{M}_{\parallel}^3 \sin 3\theta}{v^3} \frac{\mathcal{M}_z E_F^3 (E_F^2 - \mathcal{M}_z^2)}{(3E_F^2 + \mathcal{M}_z^2)^3}. \end{aligned} \quad (21)$$

$$\text{Class C : } \sigma_{xy, V_x}^{sk} = \frac{e^2}{h} \frac{u_1^3}{n_i u_0^4} \frac{\lambda E_F \mathcal{M}_{\parallel}^2 \sin 2\theta}{v^3}. \quad (22)$$

$$\sigma_{xy, V_y}^{sk} = \frac{e^2}{h} \frac{u_1^3}{n_i u_0^4} \frac{\lambda E_F \mathcal{M}_{\parallel}^2 \cos 2\theta}{v^3}. \quad (23)$$

The skew scattering contribution of each class impurity is dependent on the $r = (n_i u_1^3)^{2/3} / (n_i u_0^2)$ and is inversely proportional to the impurity density. In high mobility conductors, the skew scattering part could dominant over both the intrinsic and side jump parts, such as the Kagome metals [40]. Similar to the results in Ref. [31], the skew scattering corrections in class A and class B respect the C_{3v} symmetry. But in class C, the skew scattering contribution becomes quadratic in \mathcal{M}_{\parallel} with a π period, indicating the breaking of C_{3v} symmetry.

Let us understand the unusual angle-dependence of extrinsic AHE due to the magnetic scatterings. In the presence of magnetic impurity scatterings, the Onsager relation could be

$$\sigma_{\alpha\beta}^A(\mathbf{M}, \mathbf{u}) = -\sigma_{\alpha\beta}^A(-\mathbf{M}, -\mathbf{u}),$$

where \mathbf{M} is the direction vector of magnetic field or magnetization and \mathbf{u} denotes the direction vector of magnetic

impurity. The Onsager relation excludes all the even order terms of the total order of the magnetic impurity strength and magnetic fields. Since the skew scattering is proportional to the odd order of magnetic impurity strength, the Hall conductivity should be proportional to the zero order and even order of total magnetic field, such as $u_1^3/n_i u_0^4$ and $(u_1^3/n_i u_0^4) \mathcal{M}_\parallel^2 \sin 2\theta$. Note that the in-plane magnetic scatterings (class C) lowers the crystal symmetry and results in side jump contribution proportional to $\mathcal{M}_\parallel \sin(\theta)$ in Eqs. (18, 19).

D. Total anomalous Hall conductivity

We collect both the intrinsic and extrinsic parts and reach the total anomalous Hall conductivity for each universality class $\sigma_{xy} = \sigma_{xy}^{in} + \sigma_{xy}^{sj} + \sigma_{xy}^{sk}$:

Class A :

$$\begin{aligned} \sigma_{xy, V_0} = & -\frac{e^2}{h} \frac{4E_F \mathcal{M}_z (E_F^2 + \mathcal{M}_z^2)}{(E_F^2 + 3\mathcal{M}_z^2)^2} - \frac{e^2}{h} \frac{4\lambda \mathcal{M}_\parallel^3 \sin 3\theta}{v^3 E_F} \\ & \times \frac{E_F^2 (E_F^4 - 6E_F^2 \mathcal{M}_z^2 - 3\mathcal{M}_z^4)}{(E_F^2 + 3\mathcal{M}_z^2)^3} \\ & - \frac{e^2}{h} \frac{u_1^3}{n_i u_0^4} \frac{(E_F^2 - \mathcal{M}_z^2)}{(E_F^2 + 3\mathcal{M}_z^2)^2} [\mathcal{M}_z (E_F^2 - \mathcal{M}_z^2) \\ & + \frac{\lambda \mathcal{M}_\parallel^3 \sin 3\theta}{v^3} (E_F^4 - 14E_F^2 \mathcal{M}_z^2 - 3\mathcal{M}_z^4)]. \end{aligned} \quad (24)$$

Class B :

$$\begin{aligned} \sigma_{xy, V_z} = & -\frac{e^2}{h} \frac{4E_F \mathcal{M}_z (E_F^2 + \mathcal{M}_z^2)}{(3E_F^2 + \mathcal{M}_z^2)^2} - \frac{e^2}{h} \frac{4\lambda \mathcal{M}_\parallel^3 \sin 3\theta}{v^3 E_F} \\ & \times \frac{E_F^2 (3E_F^4 + 6E_F^2 \mathcal{M}_z^2 - \mathcal{M}_z^4)}{(3E_F^2 + \mathcal{M}_z^2)^3} \\ & + \frac{e^2}{h} \frac{u_1^3}{n_i u_0^4} \frac{(E_F^2 - \mathcal{M}_z^2)}{(3E_F^2 + \mathcal{M}_z^2)^2} [E_F (E_F^2 - \mathcal{M}_z^2) \\ & - \frac{16\lambda \mathcal{M}_\parallel^3 \sin 3\theta}{v^3} \mathcal{M}_z E_F^3]. \end{aligned} \quad (25)$$

Class C :

$$\sigma_{xy, V_x} = -\frac{e^2 \lambda E_F}{h} \left(\frac{2\mathcal{M}_\parallel \sin \theta}{v^3} - \frac{u_1^3}{n_i u_0^4} \frac{\mathcal{M}_\parallel^2 \sin 2\theta}{v^3} \right). \quad (26)$$

$$\sigma_{xy, V_y} = \frac{e^2 \lambda E_F}{h} \left(\frac{2\mathcal{M}_\parallel \sin \theta}{v^3} + \frac{u_1^3}{n_i u_0^4} \frac{\mathcal{M}_\parallel^2 \cos 2\theta}{v^3} \right). \quad (27)$$

Let us summarize several salient features here. First of all, since the scattering in class A and class B respect the C_{3v} symmetry, the anomalous Hall conductivity merely has the threefold symmetric part. Second, in the class C, the in-plane spin flipping scattering further lowers the

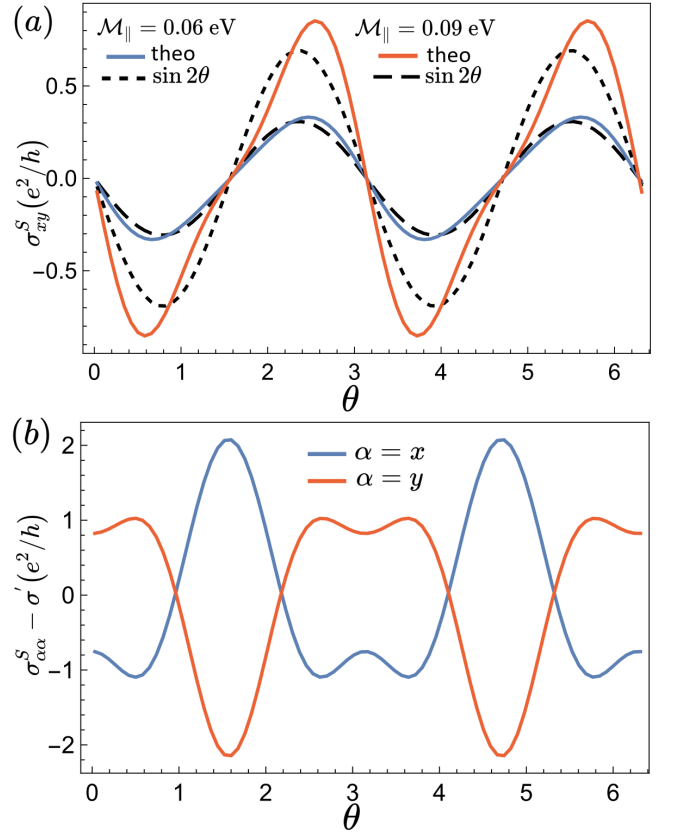


Figure 4. (a) Comparison between the calculated planar Hall conductivity and approximate one ($\sin 2\theta$ part in Eq. (30)) for two magnitudes of the in-plane magnetization. (b) The longitudinal conductivities $\sigma_{\alpha\alpha}^S - \sigma'$ with $\mathcal{M}_\parallel = 0.12$ eV. Other parameters are $\lambda = 0.01$ eV nm³, $v = 0.2$ eV nm, $E_F = 0.2$ eV, $\tau = 2$ ps.

symmetry and thus give rise to the nonzero π and 2π periodic anomalous Hall conductivity, which is distinct from the isotropic massive Dirac fermions with vanishing skew scattering contribution [31]. Third, in class B, there exists an unusual skew scattering contribution that is independent of the in-plane and out-of-plane magnetizations ($\sigma_{xy, V_z}^{sk} \approx \frac{e^2}{h} \frac{u_1^3 E_F}{9n_i u_0^4}$ from the first line of Eq. (21) in the limit of vanishing \mathcal{M}_z). It may originate from the gap renormalization induced by the disorders V_z . Note that in the limit of $\lambda \rightarrow 0$ or $\mathcal{M}_z \rightarrow 0$, our results could recover the previous ones [31, 41]. In sum, the crystal symmetry such as C_{3v} here greatly enrich the features of AHE in the presence of different classes of disorder scatterings.

V. IN-PLANE MAGNETOCONDUCTIVITY

In order to understand some puzzling magnetotransport phenomena in topological materials, we briefly discuss the impact of different classes of impurity scatter-

ings on in-plane magnetoconductivity. It is instructive to decompose the electric conductivity tensor into the symmetric and antisymmetric parts:

$$\sigma_{\alpha\beta}(\mathcal{M}) = \sigma_{\alpha\beta}^S(\mathcal{M}) + \sigma_{\alpha\beta}^A(\mathcal{M}), \quad (28)$$

where the antisymmetric part $\sigma_{\alpha\beta}^A = \frac{\sigma_{\alpha\beta} - \sigma_{\beta\alpha}}{2}$ reflects the dissipationless nature of the AHE. The symmetric part of the off-diagonal components of electric conductivity $\sigma_{\alpha\beta}^S = \frac{\sigma_{\alpha\beta} + \sigma_{\beta\alpha}}{2}$ is usually related to the planar Hall effect and has the essential nature of anisotropic magnetoresistance. In order to gain a comprehensive understanding of the role of the universal classes of scatterings in electric transport, we would like to further calculate the symmetric part of conductivity by using the Kubo formula. For the coexistence of the scalar impurities and magnetic impurities (leading order in λ) [See Sec. D of Supplemental Material [44]],

$$\sigma_{xy, V_i}^S = \frac{e^2}{h} \frac{2\lambda \mathcal{M}_{\parallel} \cos \theta \mathcal{M}_z}{v n_i u_0^2} \gamma_{V_i}, \quad (29)$$

with $\gamma_{V_0} = 3(E_F^2 - \mathcal{M}_z^2)(E_F^2 - 9\mathcal{M}_z^2)/(E_F^2 + 3\mathcal{M}_z^2)$, $\gamma_{V_z} = -3(E_F^2 - \mathcal{M}_z^2)(7E_F^2 + \mathcal{M}_z^2)/(3E_F^2 + \mathcal{M}_z^2)^2$ and $\gamma_{V_x} = \gamma_{V_y} = -5$, where γ_{V_i} is the dimensionless coefficient produced by velocity correction under different impurity classes, which is only related to the out-of-plane magnetic field. The sign of this magnetoconductivity solely depends on the direction of the in-plane magnetic field, and it has mirror-y symmetry.

In order to understand the recent planar Hall experiments, we would study the in-plane magnetoconductivity in the presence of the only in-plane magnetic field in the Kubo formula approach. One keeps all terms in the lowest order of the hexagonal warping λ and has σ_{xy}^S

$$\begin{aligned} \sigma_{xy, V_0}^S = \sigma_{xy, V_z}^S &= -\frac{e^2}{h} \frac{\lambda^2 \mathcal{M}_{\parallel}^2}{v^4 n_i u_0^2} \left(\frac{9}{2} E_F^2 \sin 2\theta \right. \\ &\quad \left. + \frac{9}{4} \mathcal{M}_{\parallel}^2 \sin 2\theta + \frac{27}{4} \mathcal{M}_{\parallel}^2 \sin 4\theta \right), \\ \sigma_{xy, V_x}^S = \sigma_{xy, V_y}^S &= -\frac{e^2}{h} \frac{\lambda^2 \mathcal{M}_{\parallel}^2}{v^4 n_i u_0^2} \left(\frac{9}{2} E_F^2 \sin 2\theta \right. \\ &\quad \left. + \frac{15}{4} \mathcal{M}_{\parallel}^2 \sin 2\theta + \frac{33}{4} \mathcal{M}_{\parallel}^2 \sin 4\theta \right). \end{aligned} \quad (30)$$

One can see that, in Fig. 4(a), our analytical theory could offer an alternative explanation of some unexplained features of the longitudinal magnetoresistance (noticeable deviation from the conventional part oscillating as $\sin(2\theta)$ (dashed lines)) in Sn doped topological insulator $\text{Bi}_{1.1}\text{Sb}_{0.9}\text{Te}_2\text{S}$ [41, 49]. Similarly, we remain the parts linear in λ and have the longitudinal conductivities $\sigma_{\alpha\alpha}^S$ as

$$\sigma_{\alpha\alpha, V_0}^S = \sigma' + \frac{e^2}{h} \frac{\lambda^2 \mathcal{M}_{\parallel}^2}{v^4 n_i u_0^2} \frac{1}{4} \left(\frac{4\mathcal{M}_{\parallel}^4 \cos 6\theta}{E_F^2} \right.$$

$$\left. -9 \left(\mathcal{M}_{\parallel}^2 + 2E_F^2 \right) \cos 2\theta + 27\mathcal{M}_{\parallel}^2 \cos 4\theta \right), \quad (32)$$

$$\begin{aligned} \sigma_{yy, V_0}^S &= \sigma' + \frac{e^2}{h} \frac{\lambda^2 \mathcal{M}_{\parallel}^2}{v^4 n_i u_0^2} \frac{1}{4} \left(\frac{4\mathcal{M}_{\parallel}^4 \cos 6\theta}{E_F^2} \right. \\ &\quad \left. +9 \left(\mathcal{M}_{\parallel}^2 + 2E_F^2 \right) \cos 2\theta - 27\mathcal{M}_{\parallel}^2 \cos 4\theta \right), \end{aligned} \quad (33)$$

where $\sigma' = [e^2 \lambda^2 (-2\mathcal{M}_{\parallel}^6 + 5E_F^6 + 27\mathcal{M}_{\parallel}^2 E_F^4 + 9E_F^2 \mathcal{M}_{\parallel}^4) + E_F^2 2v^6] / (2h E_F^2 v^4 n_i u_0^2)$ is independent of the magnetic field direction. We only consider the scattering process without velocity correction, the corresponding relaxation time is $\hbar/(2\tau) \simeq n_i u_0^2 E_F / (4v^2)$. It should be emphasized that the analytical σ_{xx}^S and σ_{yy}^S above as well as the result in Fig. 4(b) could capture the key feature of the numerical result of anisotropic magnetoconductivity of the Dirac surface states with hexagonal warping term in [50], a superposition of contributions with π period and $\pi/2$ period. That is, the hexagonal warping term offers a new mechanism for the fourfold symmetric anisotropic in-plane magnetoresistance that is distinct from that due to the topological orbital magnetic moment of Dirac fermions [51]. Thus, our theory enables us to well understand the relevant magnetotransport experiments.

VI. CONCLUSIONS AND DISCUSSIONS

In summary, we mainly explored the extrinsic part of IPAHE based on the 2D massive Dirac fermions with warping term. The distinct behaviors of IPAHE against the three universal classes of disorder scatterings are consistent with previous results of massive Dirac fermions in two limits. Notably, the spin-flipping scattering could induce extrinsic contributions of sinusoidal oscillation with periods of π and 2π , in contrast to the standard 2D massive Dirac fermions. In addition, we briefly calculated the in-plane magnetoresistance and made some comparison with previous results. Our work could provide a comprehensive picture of IPAHE under general spin-dependent scatterings and help us to understand the Hall transport of the quantum materials.

Our theory could be extended to other Berry curvature related anomalous transport effects in planar Hall geometry such as anomalous Nernst effect and thermal Hall effect in a large variety of magnetic materials that are not limited to trigonal crystals.

The authors thank Yang Gao and C. M. Wang for insightful discussions. This work was financially supported by the National Key R&D Program of the MOST of China (Grant No. 2024YFA1611300), the National Natural Science Foundation of China under Grants (No. U2032164 and No. 12174394). J.Z. was also supported by HFIPS Director's Fund (Grants No. YZJJQY202304 and No. BJPY2023B05), Anhui Provincial Major S&T

Project (s202305a12020005) and the Basic Research Program of the Chinese Academy of Sciences Based on Major Scientific Infrastructures (grant No. JZHKYPT-2021-08) and the High Magnetic Field Laboratory of Anhui Province under Contract No. AHM-FX-2020-02.

* taoqin@ahu.edu.cn

† jhzhou@hmf.ac.cn

- [1] N. Nagaosa, J. Sinova, S. Onoda, A. H. MacDonald, and N. P. Ong, *Rev. Mod. Phys.* **82**, 1539 (2010).
- [2] Y. Zhang and C. Zhang, *Phys. Rev. B* **84**, 085123 (2011).
- [3] X. Liu, H.-C. Hsu, and C.-X. Liu, *Phys. Rev. Lett.* **111**, 086802 (2013).
- [4] Y. Ren, J. Zeng, X. Deng, F. Yang, H. Pan, and Z. Qiao, *Phys. Rev. B* **94**, 085411 (2016).
- [5] Z. Liu, G. Zhao, B. Liu, Z. F. Wang, J. Yang, and F. Liu, *Phys. Rev. Lett.* **121**, 246401 (2018).
- [6] J.-Y. You, C. Chen, Z. Zhang, X.-L. Sheng, S. A. Yang, and G. Su, *Phys. Rev. B* **100**, 064408 (2019).
- [7] J. Zhang, Z. Liu, and J. Wang, *Phys. Rev. B* **100**, 165117 (2019).
- [8] J. Ge, D. Ma, Y. Liu, H. Wang, Y. Li, J. Luo, T. Luo, Y. Xing, J. Yan, D. Mandrus, H. Liu, X. C. Xie, and J. Wang, *National Science Review* **7**, 1879 (2020).
- [9] V. A. Zyuzin, *Phys. Rev. B* **102**, 241105 (2020).
- [10] J. H. Cullen, P. Bhalla, E. Marcellina, A. R. Hamilton, and D. Culcer, *Phys. Rev. Lett.* **126**, 256601 (2021).
- [11] H. Tan, Y. Liu, and B. Yan, *Phys. Rev. B* **103**, 214438 (2021).
- [12] J. Zhou, W. Zhang, Y.-C. Lin, J. Cao, Y. Zhou, W. Jiang, H. Du, B. Tang, J. Shi, B. Jiang, X. Cao, B. Lin, Q. Fu, C. Zhu, W. Guo, Y. Huang, Y. Yao, S. S. P. Parkin, J. Zhou, Y. Gao, Y. Wang, Y. Hou, Y. Yao, K. Suenaga, X. Wu, and Z. Liu, *Nature* **609**, 46 (2022).
- [13] Z. Li, Y. Han, and Z. Qiao, *Phys. Rev. Lett.* **129**, 036801 (2022).
- [14] J. Cao, W. Jiang, X.-P. Li, D. Tu, J. Zhou, J. Zhou, and Y. Yao, *Phys. Rev. Lett.* **130**, 166702 (2023).
- [15] T. Kurumaji, *Phys. Rev. Res.* **5**, 023138 (2023).
- [16] F. Xue, Y. Hou, Z. Wang, Z. Xu, K. He, R. Wu, Y. Xu, and W. Duan, *National Science Review*, nwad151 (2023).
- [17] W. Miao, B. Guo, S. Stemmer, and X. Dai, *Phys. Rev. B* **109**, 155408 (2024).
- [18] D. Xiao, M.-C. Chang, and Q. Niu, *Rev. Mod. Phys.* **82**, 1959 (2010).
- [19] Y. Cui, Z. Li, H. Chen, Y. Wu, Y. Chen, K. Pei, T. Wu, N. Xie, R. Che, X. Qiu, Y. Liu, Z. Yuan, and Y. Wu, *Science Bulletin* **69**, 2362 (2024).
- [20] H. Wang, Y.-X. Huang, H. Liu, X. Feng, J. Zhu, W. Wu, C. Xiao, and S. A. Yang, *Phys. Rev. Lett.* **132**, 056301 (2024).
- [21] L. Liu, A. Pezo, D. G. Ovalle, C. Zhou, Q. Shen, H. Chen, T. Zhao, W. Lin, L. Jia, Q. Zhang, H. Zhou, Y. Yang, A. Manchon, and J. Chen, *Nano Letters* **24**, 733 (2024).
- [22] W. Peng, Z. Liu, H. Pan, P. Wang, Y. Chen, J. Zhang, X. Yu, J. Shen, M. Yang, Q. Niu, Y. Gao, and D. Hou, (2024), 2402.15741 [cond-mat.mtrl-sci].
- [23] Z. Liu, M. Wei, D. Hou, Y. Gao, and Q. Niu, (2024), arXiv:2408.08810 [cond-mat.mtrl-sci].
- [24] A. Nakamura, S. Nishihaya, H. Ishizuka, M. Kriener, Y. Watanabe, and M. Uchida, *Phys. Rev. Lett.* **133**, 236602 (2024).
- [25] R.-C. Xiao, H. Li, H. Han, W. Gan, M. Yang, D.-F. Shao, S.-H. Zhang, Y. Gao, M. Tian, and J. Zhou, (2024), arXiv:2411.10147 [cond-mat.mtrl-sci].
- [26] P. A. Lee and T. V. Ramakrishnan, *Rev. Mod. Phys.* **57**, 287 (1985).
- [27] J. Smit, *Physica* **21**, 877 (1955).
- [28] L. Berger, *Phys. Rev. B* **2**, 4559 (1970).
- [29] N. A. Sinitsyn, A. H. MacDonald, T. Jungwirth, V. K. Dugaev, and J. Sinova, *Phys. Rev. B* **75**, 045315 (2007).
- [30] T. S. Nunner, G. Zaránd, and F. von Oppen, *Phys. Rev. Lett.* **100**, 236602 (2008).
- [31] S. A. Yang, H. Pan, Y. Yao, and Q. Niu, *Phys. Rev. B* **83**, 125122 (2011).
- [32] H.-Z. Lu and S.-Q. Shen, *Phys. Rev. B* **88**, 081304 (2013).
- [33] W.-Y. Shan, H.-Z. Lu, and D. Xiao, *Phys. Rev. B* **88**, 125301 (2013).
- [34] A. A. Burkov, *Phys. Rev. Lett.* **113**, 187202 (2014).
- [35] I. A. Ado, I. A. Dmitriev, P. M. Ostrovsky, and M. Titov, *Phys. Rev. Lett.* **117**, 046601 (2016).
- [36] E. J. König and A. Levchenko, *Phys. Rev. Lett.* **118**, 027001 (2017).
- [37] J.-X. Zhang and W. Chen, *Phys. Rev. B* **107**, 214204 (2023).
- [38] S.-Y. Yang, Y. Wang, B. R. Ortiz, D. Liu, J. Gayles, E. Derunova, R. Gonzalez-Hernandez, L. Šmejkal, Y. Chen, S. S. P. Parkin, S. D. Wilson, E. S. Toberer, T. McQueen, and M. N. Ali, *Science Advances* **6**, eabb6003 (2020).
- [39] F. H. Yu, T. Wu, Z. Y. Wang, B. Lei, W. Z. Zhuo, J. J. Ying, and X. H. Chen, *Phys. Rev. B* **104**, L041103 (2021).
- [40] G. Zheng, C. Tan, Z. Chen, M. Wang, X. Zhu, S. Albarakati, M. Algarni, J. Partridge, L. Farrar, J. Zhou, W. Ning, M. Tian, M. S. Fuhrer, and L. Wang, *Nature Communications* **14**, 678 (2023).
- [41] C. M. Wang, Z. Z. Du, H.-Z. Lu, and X. C. Xie, *Phys. Rev. B* **108**, L121301 (2023).
- [42] L. Fu, *Phys. Rev. Lett.* **103**, 266801 (2009).
- [43] S. Sun, H. Weng, and X. Dai, *Phys. Rev. B* **106**, L241105 (2022).
- [44] See Supplemental Material for details of calculations of intrinsic anomalous Hall conductivity, the extrinsic contributions in both the spin basis and eigenstate basis as well as the in-plane magnetoconductivity.
- [45] S.-Q. Shen, *Topological Insulators: Dirac Equation in Condensed Matters* (Springer-Verlag, Berlin, 2013).
- [46] W. Li and C. M. Wang, *Journal of Physics: Condensed Matter* **36**, 205001 (2024).
- [47] H. Bruus and K. Flensberg, *Many-Body Quantum Theory in Condensed Matter Physics: An Introduction*, Oxford Graduate Texts (OUP Oxford, 2004).
- [48] P. Streda, *Journal of Physics C: Solid State Physics* **15**, L717 (1982).
- [49] B. Wu, X.-C. Pan, W. Wu, F. Fei, B. Chen, Q. Liu, H. Bu, L. Cao, F. Song, and B. Wang, *Applied Physics Letters* **113**, 011902 (2018).
- [50] R. S. Akhyanov and A. L. Rakhmanov, *Phys. Rev. B* **97**, 075421 (2018).
- [51] D. Tu, C. Wang, and J. Zhou, (2024), 2402.01470.